Susceptor-assisted induction curing behaviour of a two component epoxy paste adhesive for aerospace applications

Severijns, C.; de Freitas, S. Teixeira; Poulis, J. A.

DOI
10.1016/j.ijadhadh.2017.03.005

Publication date
2017

Document Version
Accepted author manuscript

Published in
International Journal of Adhesion and Adhesives

Susceptor-assisted induction curing behaviour of a two component epoxy paste adhesive for aerospace applications

C. Severijns[a], S. Teixeira de Freitas[a,*], J.A. Poulis[a]

[a]*Delft University of Technology, Kluyverweg 1, 2629 HS Delft, The Netherlands*

Abstract

The curing behaviour and the mechanical behaviour of susceptor-assisted induction-cured adhesively bonded joints has been investigated. Induction Heating (IH) was established by mixing Iron particles into a two component epoxy paste adhesive. The effect of different process parameters, such as particle content, coupling distance and coil current, on the IH curing process was evaluated by experimental tests and simulation of the induction heating process in COMSOL multiphysics. The process simulation showed that hysteresis losses has a major contribution for the heat generation of IH using Iron particles. Differential scanning calorimetry (DSC) analysis was used to assess the effect of susceptor particles on the cure behaviour of the adhesive. The results showed that the Iron particles do not interfere with the curing process of the epoxy adhesive in scope.

The mechanical performance was evaluated through Single Lap-Shear (SLS) testing at different volume-percentages of Iron particles in combination with glass fibre reinforced plastic (GFRP) adherends. Induction-cured SLS samples were compared with conventional oven-cured SLS samples. In the oven cured samples, the addition of Iron particles resulted in a decrease in the lap-shear strength of 15% to 20%, even for a volume-percentage as low as 0.5%. An additional increase in particle content up to 7.5v% did not show any additional reduction in the lap-shear strength. Furthermore, results show that when curing the adhesive layer from the inside, as in the susceptor-assisted induction heating, the lap-shear strength is 6% higher than in oven-cured samples (curing the adhesive layer from the outside).

Keywords:

Adhesive bonding, induction curing, out-of-autoclave, Iron particles

1. Introduction

The autoclave curing process is known to be the current manufacturing technique that provides the best quality of composite laminates and adhesively bonded joints in aerospace application. However, this process implies a high acquisition cost, high energy consumption and, hence, a large ecological footprint. Furthermore, with the current composite aircraft fuselages, it is infeasible to use autoclave/oven curing processes to assemble large sections of an aircraft. Therefore, new manufacturing solutions must be developed in order to make composites and composite bonding cost-attractive, energy-efficient and applicable to large-scale assemblies, while delivering at least the same product quality as the current autoclave/oven processes. This research addresses the challenge to explore an out-of-autoclave alternative curing process for adhesively bonded joints, based on Induction Heating (IH).

The principles of the IH theory have first been established by Michael Faraday [1]. By exposing a material to an alternating electromagnetic field, heat is generated either by Joule- or hysteresis heating. The latter requires the material to be ferromagnetic for hysteresis losses to occur. Joule heating on the other hand, based on generated Eddy currents, requires the material to be conductive. In comparison with other heat transfer methods, the IH technique's main advantages are high energy transfer intensity and low energy consumption [2, 3].

As common paste adhesives are neither conductive nor magnetic, strategies have to be developed in order to apply induction heating on adhesively bonded joints. When working with conductive materials, such as aluminium or carbon fibre reinforced plastic (CFRP), heat can be generated by induction within the adherend, which is then conductively transferred to the bond layer. This is called susceptorless induction heating.

Sanchez C. et al. have established an induction curing process using CFRP adherends and a two-component epoxy paste adhesive [4–6]. Sanchez' curing process showed a reduction in energy consumption of approximately 25% when compared to conventional oven-curing, without any significant decrease in the mechanical performance of the adhesive. However, such an induction heating process is strongly dependent on the quality of the CFRP adherends in terms of fiber alignment, lay- up and manufacturing, which can significantly compromise the quality of the bonded joint. Furthermore, such curing process are limited to conductive adherends.

*s.teixeiradefreitas@tudelft.nl

If non-conductive adherends are used, such as Glass Fiber Reinforced Polymers, the adhesive can be modified in order to be able to generate heat by induction, so-called susceptor-assisted induction heating. This manufacturing has some interesting advantages over conventional oven-curing and susceptorless induction curing. First, it allows the application of induction curing on adhesively bonded joints having non-conductive adherends. Secondly, it provides the ability to generate heat locally, reducing the overall thermal stresses that occur when the complete structure needs to be heated (such as in an autoclave or oven process). Lastly, the fast increase of temperature within the bondline could enhance gas liberation, possibly resulting in a redution of void formation and thus improved mechanical performance of adhesively bonded joints.

However, susceptor-assisted IH requires that the bondline has conductive or magnetic properties, by adding either a mesh or particles. Rudolf (2000) has established a susceptor-assisted induction curing process by adding a steel mesh to the bondline [7]. However, poor adhesion between the mesh and the adhesive resulted in a reduced mechanical performance of the joint. A different strategy, used today in biomedical applications for cancer treatments, is to mix ferromagnetic nano-particles within the material to be heated, which generates heat through hysteresis losses of the particles [8]. Research has shown that different susceptor particles show different heating characteristics [9]. Also susceptor-size and weight percentage have a significant impact [10, 11]. In general, smaller sizes and higher particle content increase heat generation. Several studies also investigated the effect of adding different nano-particles on the performance of epoxy resins or adhesives. In general, the lap shear strength and peel strength increase to small amounts of particle content ($< 5 wt\%$), but a further increase in the particle content leads to a decrease in lap shear strength [12–15]. However, research is mostly focused in using the particles to reinforce the adhesive or composite resin. Few studies have been found on using the particles for IH curing. One of them is Hartwig (2009) which investigates selective heating of adhesives using superparamagnetic nano particles. The study shows that the heating rate increases with the adhesive thickness and decreases with the thermal conductivity of the adherends. The best heating rate was obtained with Glass fiber Reinforced Polymers (GFRP) when compared to polycarbonate.

Despite having the mentioned advantages and showing promising results, susceptor-assisted IH adhesive bonding is yet to be established in aerospace industry as a reliable and cost-effective alternative to autoclave/oven curing. A study which compares oven-cured with susceptor assisted

IH-curing for aerospace application is still missing.

The purpose of this research is to develop additional insights in the field of susceptor-assisted, induction-heated adhesive bonding using an aerospace certified epoxy adhesive. The aim is to assess the impact of susceptor-assisted induction heating on the curing of the epoxy and on the mechanical performance of composite bonded joints. The conventional oven curing process will be used as reference.

2. Materials and Specimens

2.1. Materials

The structural adhesive used for this project is the two component epoxy paste adhesive EC9323-B/A produced by 3M® (St. Paul, USA). This adhesive has been selected because of its wide application within the aerospace industry. The manufacturer's recommended cure cycle for this adhesive is two hours at 65°C.

The susceptor particles are Iron particles, produced by Acros Organics, with an average size of 200 μm. These particles have been chosen because of their superior heat-generating properties compared to other susceptor materials, such as Nickel or Magnetite, as found in literature [10, 16].

Glass fibre reinforced plastic (GFRP) was used as adherend material for the lap- shear specimen. This material does not generate any heat when exposed to the electromagnetic field and thereby does not interfere with the heat generation through the susceptor particles. Aluminium or Carbon Fibre Reinforced Polymer adherends were not chosen since they would shield the iron filled adhesive from the electric field.The adherends consists of eight layers of 0°/ 90°glass fibre fabric and HEXION RIM 235 epoxy resin (E_t =3.0-3.2 GPa, σ_{tu} =65-70 MPa and ϵ_{tu} =6-8% according to Technical Data Sheet). The GFRP coupons were produced by vacuum infusion and cured at room temperature for 24 hours.

2.2. Specimens

The effect of different induction heating process parameters on the heat generation has been evaluated on coin-sized coupons of a mixture of the paste adhesive and Iron particles, as shown in Figure 2(a). The coin-sized specimens had a diameter of 27 mm and a thickness of 2.95 mm. The particle content was varied from 1 to 5v%. Susceptor particles were mixed into the

adhesive manually. Scanning Electron Microscopy was used to assess the quality of dispersion by checking the dispersion of ferrite (Fe) elements for different samples. As ferrite was not detected on samples of bare adhesive, this was considered a correct method to assess the particles dispersion. Figure 1 shows the picture obtained from the SEM of a sample containing 2v% of particles. The picture shows three ferrite concentrations which indicate the location of the ferrite particles. The concentration points have between 50 μm and 150 μm maximum size. Since the nominal size of the particles is 200 μm this suggests that each Fe concentration can be considered as one particle. Therefore, it can be concluded that there is no agglomeration of the particles (good dispersion) but there is a significant inhomogeneity on the particle size.

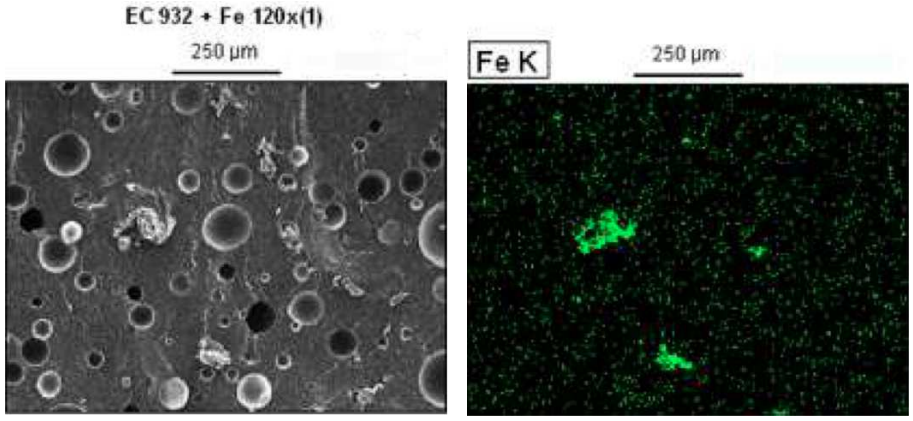

(a) SEM image (b) SEM image - Fe content

Figure 1: SEM image taken from a sample with 2v% of iron particles.

The effect on the mechanical performance was evaluated testing single lap-shear (SLS) specimens, with dimensions in accordance with ASTM standard D5868 [17]. Due to the size limitation of the available induction heating set-up, the samples were first cut into single lap-shear specimens and then assembled and cured individually. This assembly process was also implemented for the oven-cured samples to keep an identical production process for all tested coupons. The volume-percentages on the SLS specimens were varied between 0.5 and 7.5v% of Iron particles. The dimensions of the lap-shear specimens are shown in Figure 2(b). The overlap length (L) was 14.5 mm. The recommended bond layer thickness by 3M for lap-shear joints is 100 μm. However, the Iron susceptor particles used for these experiments have a size of 200 μm. This means that the susceptor- assisted lap- shear specimen would not be able to achieve a bond layer

thickness of 100 μm. Therefore 200 μm thick bond layer was used for all tested specimen, such that all test specimen would have the same dimensions. The adhesive thickness was garanteed by 200 μm glass beads mixed manually into the adhesive. If susceptor particles had to be added to the adhesive as well, this was done at the same time. This was done in order to avoid an additional mixing-stage, which could possibly increase the risk of gas formation within the adhesive. The surface of the bonding area of both GFRP specimen was carefully pretreated before the adhesive was applied. First, the surface was physically abraded with sandpaper (mesh 80) and thereafter degreased with PF-SR, a solvent made by PSG and typically used in the aerospace industry as cleaner and degreaser.

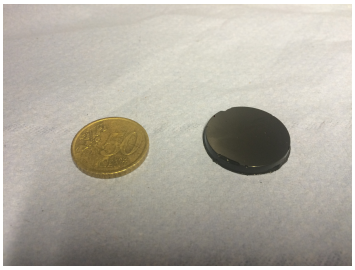

(a) Coin- sized specimen

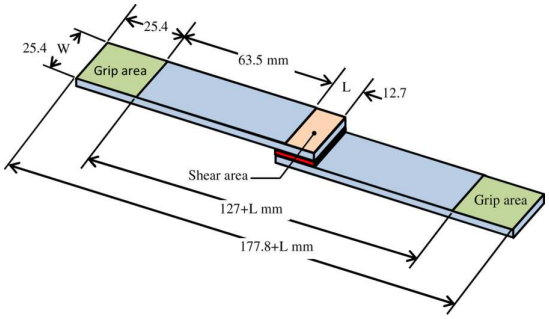

(b) Single lap- shear specimen

Figure 2: Coin- sized specimen (left) and single lap- shear specimen (right), as used in this project

3. Experimental Set-Up & Methodology

The experimental program consists of three phases. Firstly, an evaluation is made on the heat-generating characteristics of the EC9323 epoxy paste adhesive mixed with the Iron susceptor particles. Secondly, the impact of those particles on the cure chemistry of the adhesive is evaluated through DSC analysis. Both items are considered as important indicators of the cure performance of induction-heated adhesive bonding. Finally, the mechanical performance of the induction-cured adhesive is assessed by testing single lap-shear specimens.

3.1. Cure Performance

The induction heating equipment used is an EasyHeat- LE 10 kW unit, made by Ambrell. The equipment can generate magnetic fields within the frequency range of 100-400 kHz. The

strength of the induced magnetic field is controlled by altering the equipment's coil current, which can be varied up to 600 Amperes. The unit auto-tunes its field frequency, depending on the coil current and coil type used. Within the context of this research, two coil types have been used: a one-turn coil and a pancake coil. The one-turn coil resulted in a field frequency of 400 kHz, whereas the pancake coil resulted in 250 kHz. Figure 3 shows the two types of coils used (thickness 7 mm).

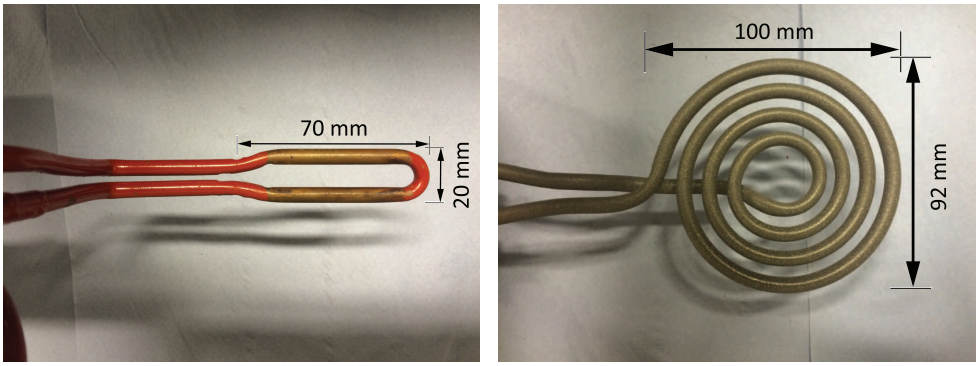

(a) One-turn coil (b) Pancake coil

Figure 3: Coil types.

The heat-generating properties have been assessed by measuring the temperature increase of the coin-sized specimens under IH. The temperatures were measured using an infra-red (IR) camera (FLIR A655sc) during a period of 200 seconds. The coin-sized specimens were placed on top of the coil set-up, in order to provide the IR camera a clear view of the heat-affected zone. The induction set-up can be seen in Figure 4.

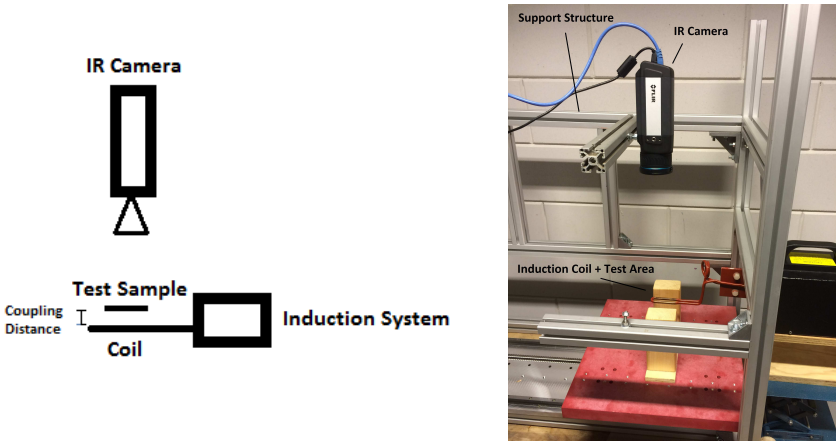

(a) Schematic overview of test set- up

(b) Actual test set- up

Figure 4: Induction Heating set-up.

The effect of four process parameters on the heating process was assessed: the influence of the volume-percentage of Iron particles, the coil current, the coupling distance and the coil type. The coupling distance is the shortest distance between the coil and the sample – see Figure 4(a). Each of these parameters was varied through its range of possible values, while all other parameters remained constant. A test matrix, including all performed test set- ups, can be found in Table 1.

Table 1: Summary of all experiments performed

Process parameter	v%	Coil current [A]	Coupling distance [mm]	Coil geometry
v%- effect	1, 2, 5	400	1	One-turn
Coil current- effect	2	100, 200, 300, 400, 500	1	One-turn
Coupling distance- effect	2	400	1, 3, 5, 7	One-turn
Coil geometry- effect	2	400	1	One-turn, pancake

The effect of the mixed-in Iron particles on the cure behaviour of the adhesive has been assessed through Differential Scanning Calorimetry (DSC) analysis. Samples were cured for two hours at 65°C while their heat flow was monitored. The heat flow data was measured for samples of adhesive including 2v% of Iron particles, and compared to the heat flow of samples of pure adhesive (no Iron particles).

3.2. Joint Performance

In order to obtain the mechanical performance of the induction-cured adhesive, single-lap shear tests were performed according to ASTM standard D5868 [17]. The tests were performed on a Zwick International 10 kN tensile test machine at 5 mm/min testing speed – displacement controlled. Three sets of lap- shear coupons have been produced, as summarized in Table 2. For each series a minimum of three specimens were tested.

Table 2: Test matrix for the single lap- shear tests

	Curing method	v%
Test series 1: Oven - no particles	Oven	-
Test series 2: Oven - with particles	Oven	0.5, 2, 5, 7.5
Test series 3: Induction - with particles	Induction	7.5

Single lap shear specimens were cured at the manufacturer's recommended cure cycle of two hours at 65°C. Oven-cured samples were cured in a Heraeus T6030 oven, after a pre-heating set to 65°C.

After an optimization study of the curing cycle via thermogravimetric analysis, it was decided to keep the curing cycles of 65°C for 120 minutes also in the IH samples. The analysis showed that using shorter curing cycles at higher temperatures, such as 110°C for 47 minutes, decreased the lap shear strength of the adhesive. Since, the aim was to keep as much as possible the same lap shear strength using IH to make it comparable to the oven curing, it was decided to keep the curing cycle 120 min at 65°C. The analysis on optimizing the curing cycles can be found in Severijns (2016) [16].

Induction-cured samples had to be manufactured with 7.5v% of Iron particles. Lowering the particle content would require too high coil currents for the induction equipment to sustain a curing process of two hours without exceeding the cooling unit's maximum temperature. The process parameters used for Induction-curing the SLS specimens were: 1 mm coupling distance; pancake coil; coil current of 6 minutes at 220 A for the heat up stage and 175 A for the remaining curing cycle.

The temperature of the SLS specimens was monitored during the complete curing process, both for the IH process and for the oven – see Figure 5. On the Induction-cured specimens thermocouples were placed inside the adhesive, at the center of the overlap. K-type thermo-

couples with 0.66 mm probe diameter were used. The measured temperatures were compared with the ones obtained from the infra-red (IR) camera, which measured the adherends surface temperature – see IR camera position in Figure 4. As shown in Figure 5, the adhesive layer is at 65°C when the infra-red camera measures 59°C at the adherend surface. As the inclusion of the thermocouples inside the adhesive layer could have an influence in the specimen's mechanical performance, the temperature of the lap-shear specimens was monitored only by the IR camera (without thermocouples), keeping as reference the 59°C temperature at the adherends surface. On the oven-cured samples, the thermocouples inside the adhesive layer showed similar temperatures as the set temperature of the oven – see Figure 5. IH takes 6 min from RT to 66°C and oven takes 8 to 9 minutes from RT to 63°C. Also interesting to observed that the heating rate, from start to target temperature, is faster in the IH setup. The oven heating rate is lower at the starting point but speeds up when temperatures are above 45 °C. This speed up allows the oven temperature to reach the target temperature shortly after the IH system.

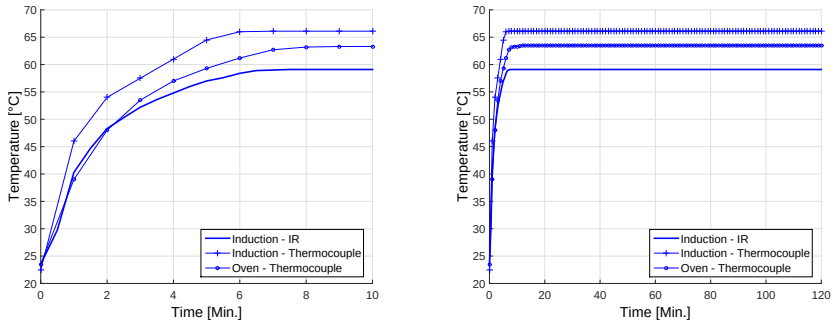

(a) Heating up (b) Heating up and hold

Figure 5: Temperature profile for the oven- and induction- cured SLS samples for two hours at 65°C.

4. Results

4.1. Cure Performance

4.1.1. Heat Generation

Figures 6 to 9 show the obtained temperature profiles for the coin specimens used for the induction heating experiments. These graphs show the effect of the volume- percentage of Iron particles (Fig. 6), the coil current (Fig. 7), the coupling distance (Fig. 8) and the coil geometry

(Fig. 9), respectively. The position of the coin-size specimens in the one illustrated in Figure 4(a).

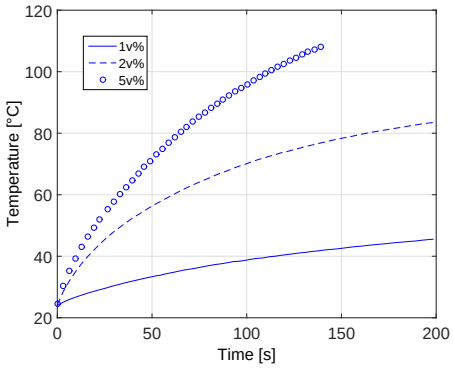

Figure 6: Temperature profiles for 1, 2 and 5v% of Iron particles (400 A, 1 mm coupling distance and one-turn coil).

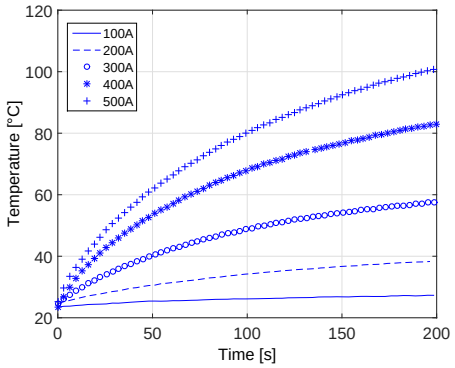

Figure 7: Temperature profiles for 100 to 500 A coil current (2v% samples, 1 mm coupling distance and one-turn coil).

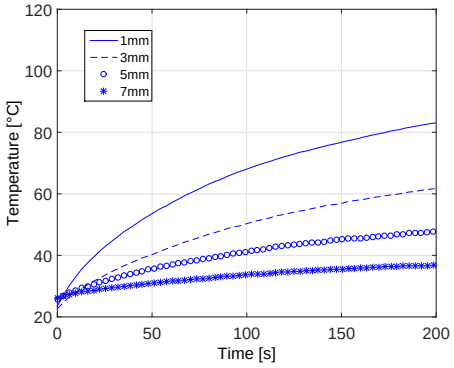

Figure 8: Temperature profiles for 1 to 7 mm coupling distance (2v% samples, 400 A and one-turn coil).

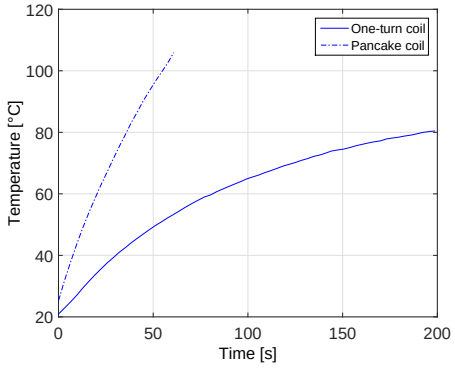

Figure 9: Temperature profiles one- turn & pancake coil (2v% samples, 400 A and 1 mm coupling distance).

Figure 6 shows that increasing the volume- percentage of Iron particles results in an increase of heat generation.

Figures 7 and 8 show that a reduction in coupling distance and/or an increase in coil current have comparable effects: an increase in temperature. These results were expected, as they both influence the magnetic field strength experienced by the susceptor particles. Both parameters

are bound by certain limitations, depending on the type of application. The achievable coupling distance will be driven by the application's size and geometry. Curing a standard single lap-shear joint by induction heating results automatically in a coupling distance equal to the size of the adherend's thickness. The allowable coil current to be applied is limited by the duration of the heating cycle, as only limited cooling power is available.

Figure 9 shows that the pancake coil generates more heat than the one-turn coil. In addition to different frequencies (pancake coil 250 kHz and one-turn coil 400 kHz), the coil geometry might change the magnetic field strength – the pancake coil has a higher number of turns and, thus, it is capable of generating a stronger magnetic field. Figures 10 and 11 show the spacial temperature distribution read from the IR camera for both coils. It can be seen that in the area within the coil, the temperature is quite uniform on both coil types. The temperature profiles shown in Figure 9 were measured in this area of uniform temperature. The shape of this uniform temperature area seems to be related with the shape of the coil. For the one-turn coil, the area has a rectangular shape while for the pancake coil it is a circle.

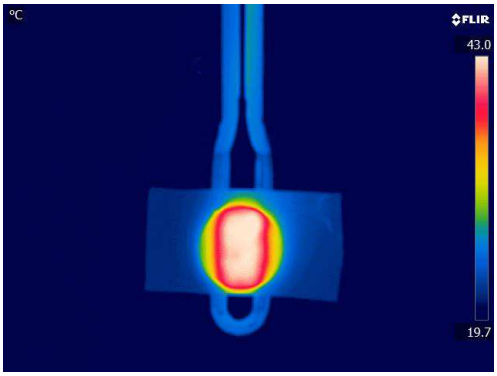

Figure 10: The heat- affected area with a one- turn coil (2v% samples, 400 A and 1 mm coupling distance)

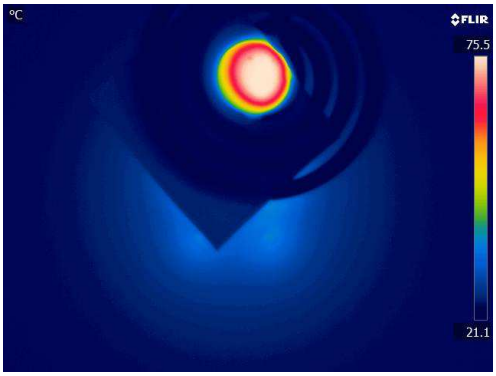

Figure 11: The heat- affected area with a pancake coil (2v% samples, 400 A and 1 mm coupling distance)

4.1.2. Cure Behaviour Analysis

Figure 12 shows the heat flow graphs obtained from the DSC experiments. Heatflow data was normalized by dividing the total measured heat flow by the sample's weight. The weight of the susceptor particles was deducted to obtain the normalized data. One can see that both samples obtain a full cure in two hours, as both graphs reach a residual heat flow after 120 min.

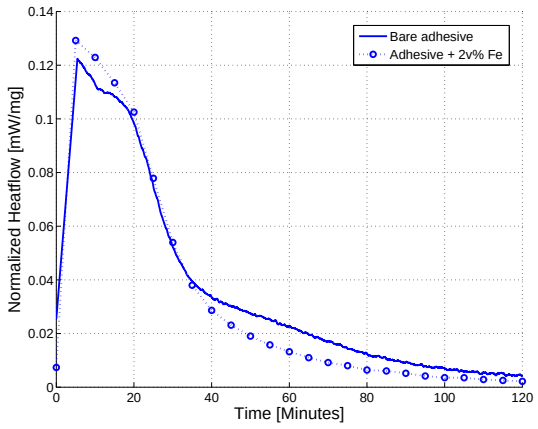

Figure 12: Heat flow curves obtained from the DSC analysis at 65°C for susceptor- assisted (2v%) and pure adhesive.

As shown in Figure 12, both the susceptor-assisted and pure adhesive show comparable heat flow trends over the curing process. Additionally, the total area underneath both curves, representing the total cure energy, is also comparable. These results show that the addition of Iron particles does not influence significantly the cure behaviour of the adhesive.

4.2. Joint Performance

Figure 13 shows the representative load- displacement curves obtained from the lap- shear tests. At the end of each test, the fracture surface of the joint has been examined in order to determine the type of failure mode. All samples showed a 100% cohesive failure in the adhesive layer. Typical examples of the fracture surfaces are shown in Figures 14 and 15 with and without Iron particles, respectively.

The effect of Iron particles on the lap-shear strength was assessed only on oven-cured samples. This was done in order to isolate the effect of the susceptor particles on the lap shear strength and avoid possible side-effects related to the induction heating process.

Induction-cured samples were manufactured with 7.5v% of Iron particles. This was the minimum % of Iron particles needed to run the Induction Heating system for two hours at a hold temperature of 65°C (coil current of 175 A).

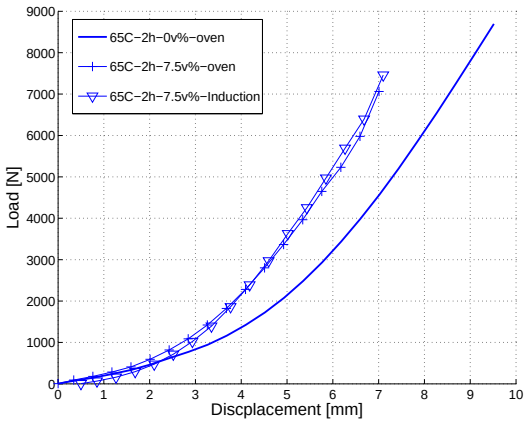

Figure 13: Representative load- displacement curves from the SLS experiments.

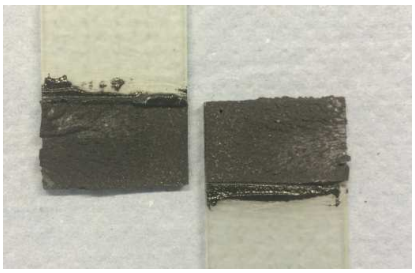

Figure 14: Example of fracture surface of a tested specimen, including 0.5v% of Iron powder and oven-cured for two hours at 65°C

Figure 15: Example of fracture surface of a tested specimen without Iron powder, oven-cured for two hours at 65°C

4.2.1. Effect of Particle Content

The average lap-shear strength for oven-cured samples with different contents of Iron particles is shown in Figure 16 and Table 3. The addition of Iron particles to the adhesive results in a reduction of lap- shear strength of approximately 15%, even at a particle content as low as 0.5v%. Increasing the particle content further up to 7.5v% does not result in a significant additional decrease in the mechanical performance of the adhesive.

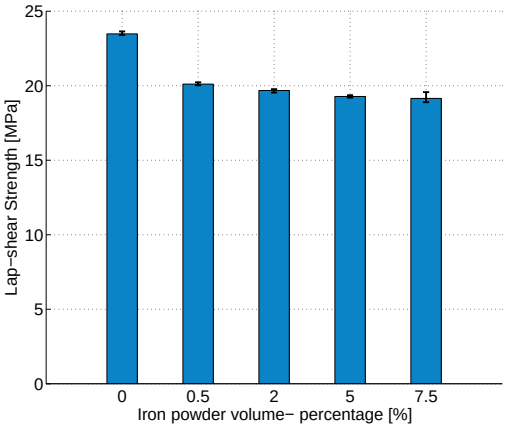

Figure 16: Average lap-shear strength of oven-cured samples with different volume-percentages of Iron particles

Table 3: Average lap-shear strength of oven-cured samples with different volume- percentages of Iron particles

Volume- percentage (v%)	0	0.5	2	5	7.5
Lap-shear strength [MPa]	23.48	20.11	19.68	19.28	19.15
St. Dev.	1%	1%	1%	0.5%	2%
Failure Mode	100% Cohesive	100% Cohesive	100% Cohesive	100% Cohesive	100% Cohesive

4.2.2. Effect of the Curing Process: Oven vs. Induction

Table 4 shows the results on the performance of induction-cured samples, containing 7.5v% of Iron particles. In comparison to oven-cured samples with the same amount of susceptor particles, the lap-shear strength of the induction-cured samples shows a slight increase of 6%. In comparison to oven-cured samples without any susceptor particles, the induction curing process results in lower mechanical performance of the adhesive. The addition of Iron particles reduces the mechanical performance, independent of the type of curing process.

Table 4: Average lap-shear strength of induction- and oven-cured samples with 7.5v% of Iron particles

Cure method	Oven	Induction
Lap- shear strength [MPa]	19.15	20.38
St. Dev.	2%	2%
Failure Mode	100% Cohesive	100% Cohesive

5. Discussion

5.1. Cure Performance

In order to better understand the obtained results, additional simulations on the induction heating process were performed.

5.1.1. Modelling of the Induction Heating Process

A model was made of the induction heating process of the coin-type specimen in COMSOL Multiphysics. Joule heating was modelled by the standard induction heating interface of COMSOL. The effect of hysteresis heating was added by the implementation of vector-hysteresis modelling, based on the Jiles-Atherton theory [19]. Figure 17 shows a schematic overview of the model as well as a model visualization.

The mixture of adhesive and Iron particles was modelled as a single uniform material with homogeneous material properties. The properties of the combined material were taken as a "rule-of-mixture" between the properties of the adhesive and the Iron particles, with a mixing ratio defined by the volume-percentage of each material.

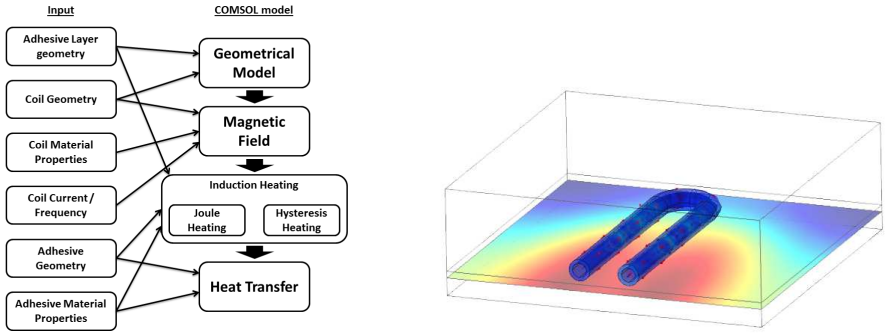

(a) Schematic overview (b) Model visualization (one-turn coil)

Figure 17: Overview of the induction heating model

The model's geometrical constraints and material parameters were established such that they represent the actual experimental set-up as close as possible. All parameter values were either found in literature or measured at the actual set-up. Table 5 summarizes the values used for simulating the induction heating process. The properties of the combined material are given

for the example of 2v% Iron powder. The electrical conductivity of the combined material was considered to be very low (similar to an isolating material).

Table 5: Induction heating model parameters.

Parameter		Value	Source
Coil current	I	400 A	As used in the lab's tests
Frequency	ω	400 KHz	As used in the lab's tests
Electrical conductivity	σ	0.01 S/m	Isolating material
Relative permeability	μ_r	4000 [-]	Iron: 200000 [25]
			Adhesive: 1 (non- magnetic)
			(Mixture: 2v% Fe + 98v% Adh.)
Relative permittivity	ϵ_r	1 [-]	Iron: -
			Adhesive: 1
			(Mixture: 2v% Fe + 98v% Adh.)
Adhesive density	ρ	1.04 g/cm^3	Product's datasheet [26]
Specific heat capacity	C_p	1300 J/($kg \cdot K$)	[18]
Thermal conductivity	k	0.72	Product's datasheet [26]

The Jiles- Atherton theory was implemented by using the governing equations as found in literature [19]. It explains hysteresis heating as a result of two phenomena: (1) heat generated through the changing magnetization of the material, called anhysteretic magnetization M_{an}; and (2) frictional heating resulting from the rotation of the material's grains, also called "wall pinning". The theory links the amount of heat generated through hysteresis losses to a set of five material parameters. The values for each of those parameters were obtained from literature, as shown in Table 6.

Table 6: Hysteresis- heating parameters [19]

Parameter	Symbol	Value	Source
Magnetic saturation	M_S	26.8×10^3 A/m	Iron: 1.3445×10^6 A/m Adhesive: 0 (non- magnetic) (Mixture: 2v% Fe + 98v% Adh.)
Langevin parameter	a	45 A/m	Iron: 2.26×10^3 A/m Adhesive: 0 (non- magnetic) (Mixture: 2v% Fe + 98v% Adh.)
Pinning factor	k	29.7 A/m	Iron: 1.4842×10^3 A/m Adhesive: 0 (non- magnetic) (Mixture: 2v% Fe + 98v% Adh.)
Domain rotation loss	c	0.7476	Iron: 0.7476 No mixture required
Shape factor	α	-0.0044	Iron: -0.0044 No mixture required

The Jiles- Atherton theory was implemented within the induction heating model according to a set of constitutive equations [20, 21]. The total amount of heat generated inside a material is calculated as a function of the domain rotation, called anhysteretic magnetization M_{an} and the irreversible magnetization due to wall pinning M_{irr}. This relation is shown in equation 1.

$$\frac{dM}{dt} = \frac{dM_{an}}{dt} + (1 - c) \cdot \frac{dM_{irr}}{dt} \tag{1}$$

The reversible magnetization $M_{an}(M_s, a)$ is determined by equation 2, by using the Langevin polynomial [22]. It depends on the magnetic saturation M_S, on the Langevin parameter a and on the effective magnetic field H_{eff}. The latter is depending on the initial magnetic field H and material's local field factor α, as shown in equation 3.

$$M_{an} = M_S \left(coth \frac{H_{eff}}{a} - \frac{a}{|H_{eff}|} \right) \frac{H_{eff}}{|H_{eff}|} \tag{2}$$

$$H_{eff} = H + \alpha \cdot M \tag{3}$$

The last element of equation 1, describing the effect of irreversible magnetization M_{irr} is determined using equation 4. This relation includes the material's pinning factor k, the domain rotation loss c and the reversible magnetization M_{rev}. The latter is calculated using equation 5.

$$\frac{dM_{irr}}{dt} = \left((k^{-1} \cdot c^{-1} \cdot M_{rev}) \cdot \frac{dH_{eff}}{dt}\right) \frac{k^{-1} \cdot c^{-1} \cdot M_{rev}}{|k^{-1} \cdot c^{-1} \cdot M_{rev}|} \tag{4}$$

$$M_{rev} = c \cdot (1 - c)^{-1} \cdot (M - M_{an}) \tag{5}$$

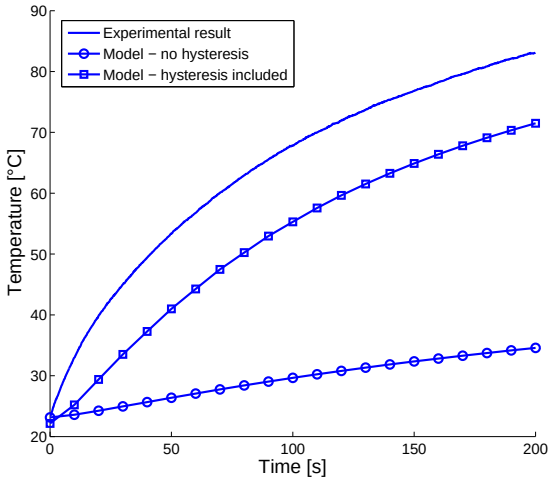

Figure 18: Simulated and experimentally obtained temperature profile for 2v%, 400 A, 1 mm coupling and the one- turn coil

Figure 18 compares the temperature profiles obtained from the experiments with the ones obtained from the COMSOL simulations. The induction heating process simulated was a 2v%-Iron adhesive sample, using 400 A coil current, a coupling distance of 1 mm and a one-turn coil. Two results from the simulations are presented: with and without hysteresis heating. When hysteresis heating is not taken into account, only a very slight increase in temperature is noticed. When hysteresis losses are taken into account, the model shows significantly higher temperature increase and simulates the induction heating process more accurately. The difference between the COMSOL simulation with hysteresis and the experiment is approximately 15%. The rule-of-mixture assumption and the values taken from literature (and not from the actual materials used),

are considered to be the main sources of error for this discrepancy. Nevertheless, the model can capture the general trend obtained in the experiments.

The results show that hysteresis losses has a major contribution for the heat generation of susceptor-assisted induction heating using Iron particles. Hysteresis losses are considered to be only a secondary heating source in induction heating theory when compared to Joule heating. This explains why CFRP susceptorless set-ups can generated significantly more heat than Iron particle susceptor-assisted set-ups [23], since the former is based on Joule heating effect and the latter on hysteresis losses. Sanchez C. has performed experiments on susceptorless set-ups, using CFRP adherends, obtaining significantly better heat generating characteristics than the susceptor-assisted set-up used in this project. Despite many parameters remaining the same, such as coupling distance and coil geometry, the CFRP set-up only required approximately 45 A to reach a temperature of 80°C [5].

5.2. Joint Performance

Previous research has focussed on the effect of susceptor particles on the lap-shear strength of bonded joints, in the context of nanoparticle reinforcement of structural adhesives [24]. The influence of such particles on the mechanical performance of adhesively bonded joints can either be positive or negative, and depends mainly on the type of susceptor material, particle size- & shape and the adherence between the susceptor particles and the adhesive. One of the most successful cases reported in a modified epoxy adhesive is using 5w% of alumina nano-particles, which showed an increase in lap-shear strength of 15% [24].

One possible explanation of the significant reduction in lap-shear strength found in the current study could be that the susceptor particles did not have a good adherence to the adhesive. However, this seems not to be the case when looking at a scanning electron microscopy (SEM) images taken from the fracture surface of tested lap- shear specimen – see Figures 19(a) and 19(b) both representing the same image. Figure 19(b) can be used to identify a representative Iron particle in the middle of the image by locating the cluster of green dots. When looking at Figure 19(a), one can see that most of the Iron particle is surrounded by (black) adhesive. This can be considered as an indication of good adhesion between the susceptor particles and the adhesive itself, since the joint's failure did not occur at the interface between the adhesive and the susceptor particles. Comparable SEM results were obtained throughout the complete joint's fracture surface.

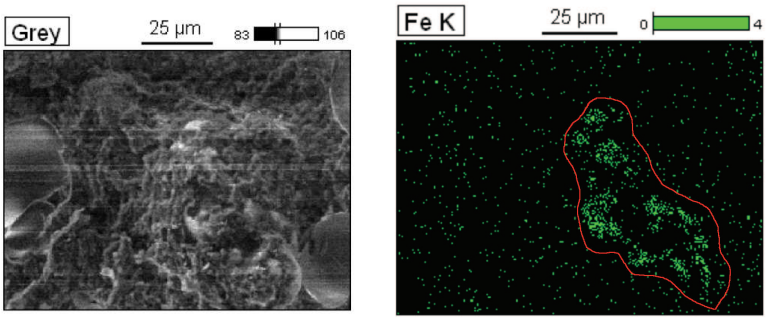

(a) SEM-photo (b) SEM-Iron content

Figure 19: SEM image of the fracture surface of a single lap-shear specimen with 7.5v% of Iron powder.

Iron powder was selected as a susceptor particle for this research mainly because of its good heat-generating characteristics, compared to the other susceptor particles previouly tested [16]. However, Iron powder shows a highly irregular particle-shape, as can be seen in Figure 20. Additionally, former research mentioned in the above paragraph made use of smaller sized nanoparticles with sizes up to 100 μm, while the Iron powder used in this research has a nominal particle size of 200 μm, although the size varied, as shown in Figure 20 ([24]. Both of those aspects might result in local distortions and stress concentrations within the adhesive, which can cause the reduction in the measured lap-shear strength. Additional concerns for using Iron powder come from durability aspects, such as corrosion.

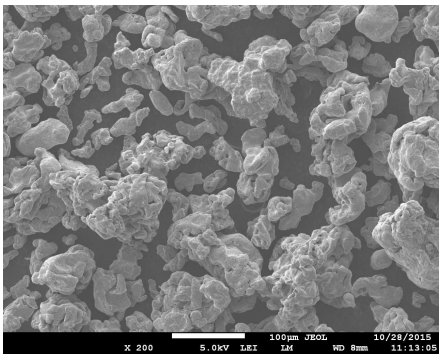

Figure 20: SEM image of the pure Iron particles used in this project.

6. Conclusions

This study evaluates the curing behaviour and mechanical performance of induction-cured bonded joints, as a possible alternative to traditional oven-cured processes. Heat was generated from the inside of the adhesive layer, by adding ferromagnetic susceptor particles to a two component paste adhesive, in order to cure bonded joints of non-conductive adherends. The main conclusions from this research are summarized as follows:

- Susceptor- assisted induction curing using Iron particles is mainly driven by hysteresis heating, which is considered only to be a secondary heating mechanism of induction heating.
- Adding Iron particles does not have any impact on the curing behaviour of the studied paste adhesive.
- Adding Iron particles to the adhesive results in a reduction of the lap-shear strength of 15%, even at a small particle content as 0.5v%. A further increase in particle content, up to 7.5v%, does not result in any additional decrease in lap-shear strength.
- Curing the adhesive layer from the inside-out, as in susceptor-assisted induction heating, results in a slight increase in lap- shear strength (6%), compared to oven-cured samples (cured from the outside-in).

Acknowledgments

This research was supported by Fokker Aerostructures.

[1] S. Lupi, M. Forzan. Induction and Direct Resistance Heating - Theory and Numerical Modelling. *Springer International Publishing Switzerland*, 2–22, 2015.

[2] D. Abliz, Y. Duan, L. Steuernagel, L. Xie, D. Li, and G. Ziegmann. Curing methods for advanced polymer composites -A review. *Journal of Polymers and Polymer Composites*, 21(6):341–348, 2013.

[3] G. Benkowsky. Induktionserwarmung Verlag Technik GmbH, 1990

[4] A. Sanchez Cebrian, R. Basler, F. Klunker, M. Zogg. Acceleration of the curing process of a paste adhesive for aerospace applications considering cure dependent void formations. *International Journal of Adhesion and Adhesives*, 48:51–58, 2013.

[5] A. Sanchez Cebrian, F. Klunker, M. Zogg. Simulation of the cure of paste adhesives by induction heating. *Journal of Composite Materials*, 8092, 2013.

[6] A. Sanchez Cebrian, M. Zogg, P. Ermanni. Methodology for optimization of the curing cycle of paste adhesives. *International Journal of Adhesion and Adhesives*, 40:112–119, 2013.

[7] R. Rudolf, P. Mitschang, M. Neitzel. Induction heating of continuous carbon-fibre-reinforced thermoplastics. *Composites Part A: Applied Science and Manufacturing*, 31:1191–1202, 2000.

[8] A. Ito, M. Shinkai, H. Honda. Medical application of functionalized magnetic nanoparticles. *Journal of bioscience and bioengineering*, 100(1):1–11, 2005.

[9] E. Verde, G. Landi, M. Carriao, A. Drummond, J. Gomes, E. Vieira, M. Sousa, A. Bakuzis. Field dependent transition to the non-linear regime in magnetic hyperthermia experiments: Comparison between maghemite, copper, zinc, nickel and cobalt ferrite nanoparticles of similar sizes. *AIP Advances*, 2(3):0–23, 2012.

[10] T. Bayerl, A. Borras, J. Gallego, B. Galiana, P. Mitschang. Melting of Polymer-Polymer Composites by Particulate Heating Promoters and Electromagnetic Radiation. *Journal of Synthetic Polymer-Polymer Composites*,39–64, 2012.

[11] D. Bae, P. Shin, S. Kwak, M. Moon, M. Shon, S. Oh, G. Kim. Heating behavior of ferromagnetic Fe particle-embedded thermoplastic polyurethane adhesive film by induction heating. *Journal of Industrial and Engineering Chemistry*,30:92–97, 2015.

[12] EN. Gilbert, BS. Hayes, JC. Seferis. Nano-alumina modified epoxy based film adhesives. *POLYMER ENGINEERING AND SCIENCE*,43(5):1096-1104, 2003.

[13] S. Meguid, Y. Sun. On the tensile and shear strength of nano-reinforced composite interfaces. *Materials and Design* 25:289296, 2004.

[14] H. Dodiuka, S. Keniga, I. Blinskya, A. Dotana, A. Buchman. Nanotailoring of epoxy adhesives by polyhedral-oligomeric-sil-sesquioxanes (POSS). *International Journal of Adhesion and Adhesives*,25(3):211-218, 2005.

[15] A. Hartwig, A. Luhring, J. Trautmann. Spheroidal Nanoparticles in Epoxide-Based Adhesives. *Macromolecular Materials and Engineering*,294(6):363-3798, 2009.

[16] C. Severijns. On the Assessment of Induction-Heated Adhesive Bonding. Master of Science Thesis, Delft University of Technology, 2016.

[17] ASTM D5868 standard. Standard Test Method for Lap Shear Adhesion for Fiber Reinforced Plastic (FRP) Bonding. 2008.

[18] Specific heat capacity measurements and using DSC specific heqt capacity measurements using DSC I. 1–4,1981.

[19] Y. Tan, Z. Zhang, J. Zu. Generalized dynamic modelling of Iron- Gallium Alloy for transducers. *Journal of Applied Mathematics and Physics*, 980–988, 2015.

[20] S. Hussain, D. Lowther. Prediction of Iron losses using Jiles- Atherton model with interpolated parameters under the conditions of frequency and compressible stress. *IEEE Transactions on Magnetics*, 52(3), 2016.

[21] S. Motoasca, G. Scutaru. Hysteresis modelling of soft magnetic materials using LabVIEW programs. *Advances in electrical and computer engineering*, 10(2):94–97, 2010.

[22] C. CepiÅca, H. Andrei, V. Dogaru-Ulieru. Evaluation of the parameters of a magnetic hysteresis model. *Journal of Materials Processing Technology*, 181(1):172–176, 2007.

[23] M. Hashmi. Comprehensive material processing, assessing properties of conventional and specialized materials. 1:491–495, 2010.

[24] C. Taylor. Advances in nanoparticle reinforcement in structural adhesives. *Woodhead Publishing Limited*, 2010.

[25] J. Davies. Induction Heating Handbook. *McGraw-Hill*, 1979.

[26] 3M Scotch-Weld. Two part structural adhesive EC-9323 B/A Aerospace Technical Data Sheet. *3M European Aerospace Laboratory*, 2013.